



## Artery Research

ISSN (Online): 1876-4401

ISSN (Print): 1872-9312

Journal Home Page: <https://www.atlantis-press.com/journals/artres>

---

### **P2.18: TOWARDS COMPUTATIONAL DIAGNOSIS OF CORONARY ARTERY DISEASE**

S. Shaw, J.R. Whiteman, S.E. Greenwald, C. Kruse, H.T. Banks, M.J. Birch, Z.R. Kenz, J. Reeves, S. Hu, M.P. Brewin

**To cite this article:** S. Shaw, J.R. Whiteman, S.E. Greenwald, C. Kruse, H.T. Banks, M.J. Birch, Z.R. Kenz, J. Reeves, S. Hu, M.P. Brewin (2013) P2.18: TOWARDS COMPUTATIONAL DIAGNOSIS OF CORONARY ARTERY DISEASE, Artery Research 7:3\_4, 123–124, DOI: <https://doi.org/10.1016/j.artres.2013.10.079>

**To link to this article:** <https://doi.org/10.1016/j.artres.2013.10.079>

Published online: 14 December 2019

left ventricular influence the carotid strain. Change in longitudinal carotid strain might serve as an early marker of cardiovascular disease.

**Table 1** Peak Longitudinal (L) and Circumferential (C) Strain (S) and Strain Rate (SR), Longitudinal (L D) and Radial (R D) Displacement of carotid arteries

L S, %	L SR	L D, mm	C S, %	C SR	RD, mm
10.8±4.1	1.5±0.6	0.45±0.1	7.8±1.7	0.8±0.17	0.27±0.6

Data is expressed as mean ± SD; L S – peak Longitudinal Strain, L SR – peak Longitudinal Strain Rate, L D – peak Longitudinal Displacement, C S – peak Circumferential Strain C SR – peak Circumferential Strain Rate, R D – peak Radial Displacement

**Table 2** Independent relations of longitudinal carotid strain with arterial stiffness and cardiac parameters

	$\beta$	P
Carotid Stiffness $\beta$	-0.49	0.03
Aortic Stiffness, $\beta$	-0.42	0.04
LV fractional shortening	0.38	0.048
relative LV posterior wall thickness	0.19	0.16
ventricular septum thickness	0.17	0.24
E/A	0.40	0.045

#### P2.14

##### COMPARISON OF AGE-RELATED CENTRAL AORTIC BLOOD PRESSURE PARAMETERS USING TWO SPHYGMOCOR TECHNIQUES

Z. Sabahi<sup>1</sup>, M. Butlin<sup>2</sup>, C. Yeung<sup>1</sup>, A.P Avolio<sup>2</sup>, E. Barin<sup>1</sup>

<sup>1</sup>Macquarie University Hospital and Clinic, Sydney, Australia

<sup>2</sup>Australian School of Advanced Medicine, Macquarie University, Sydney, Australia

**Background.** Central aortic blood pressure (CBP) parameters are increasingly proved to be stronger predictors of cardiovascular outcomes than peripheral blood pressure parameters. Aortic stiffness, which increases with age, alters these parameters. The aim of this study was to compare the CBP parameters measured by two SphygmoCor techniques: tonometric (Classic) and cuff-based (XCEL) with respect to age.

**Methods:** 186 individuals (mean age 68±45 years, range 21-93 years, 97 males) from general cardiac clinic patients were recruited. Tonometric and cuff-based assessment of central systolic blood pressure (cSBP), central diastolic blood pressure (cDBP), central pulse pressure (cPP) and augmentation index normalised to a heart rate of 75 beats/min (Alx75) was made in a randomized fashion after a period of seated acclimatization. Statistical analysis was performed by means of Analysis of Covariance (ANCOVA) with respect to device and age, with an interaction term between device and age to detect age dependent differences between devices.

**Results.** All parameters changed significantly with age ( $p < 0.001$ ). There was no significant difference between all parameters estimated by the two techniques (Table). The interaction term of device and age was not significant for any parameter, indicating that the devices did not differ with respect to age.

**Conclusion.** The new cuff-based SphygmoCor technique used for evaluation of CBP parameters in a clinical environment is a convenient and accurate proxy for the previous tonometric technique regardless of patient age.

Parameter	Device	Slope	Intercept	p		
				Device	Age	Age*device
cSBP/age (mmHg/yr)	Classic	0.28±0.07	97±5	0.49	<0.001	0.58
	XCEL	0.23±0.06	101±4			
cDBP/age (mmHg/yr)	Classic	-0.16±0.04	82±3	0.66	<0.001	0.99
	XCEL	-0.16±0.04	84±3			
cPP/age (mmHg/yr)	Classic	0.45±0.06	14±4	0.55	<0.001	0.42
	XCEL	0.39±0.05	17±3			
Alx75/age (%/yr)	Classic	0.22±0.04	6±3	0.13	<0.001	0.38
	XCEL	0.16±0.06	14±4			

#### P2.15 Withdrawn by author

#### P2.16

##### PULSE WAVE VELOCITY ASSESSED BY NON-INVASIVE TONOMETRY, IN ANESTHETIZED GÖTTINGEN MINIPIGS

T. P. Ludvigsen<sup>1</sup>, N. Wiinberg<sup>2</sup>, C. J. Jensen<sup>1</sup>, A. T. Callesen<sup>1</sup>, H. D. Pedersen<sup>3</sup>, B.Ø. Christoffersen<sup>3</sup>, L. H. Olsen<sup>1</sup>

<sup>1</sup>University of Copenhagen, Copenhagen, Denmark

<sup>2</sup>Frederiksberg Hospital, Frederiksberg, Denmark

<sup>3</sup>Novo Nordisk A/S, Måløv, Denmark

**Introduction:** Assessment of pulse wave velocity (PWV) is recognized as a marker of arterial stiffness within human medicine. Non-invasive evaluation of arterial structural changes in relation to atherosclerosis in porcine models of cardiovascular disease, would be valuable in longitudinal assessment of pathophysiological changes, e.g. in relation to drug effect.

**Objective:** To evaluate the feasibility and reproducibility of PWV in anesthetized male Göttingen minipigs.

**Method:** Animals were anesthetized every second day (three days in total) using constant intravenous infusion of ketamine and midazolam. Mean arterial blood pressure (MAP) assessed by oscillometry and heart rate (HR) were registered. PWV was calculated as the distance between the carotid and femoral artery divided by the time delay of pressure pulses, assessed by aplanation tonometry and simultaneously recorded electrocardiography (ECG).

**Results:** MAP was 87.6 mmHg ± 11.9 (mean ± SD), 80.5 mmHg ± 12.7 and 84.3 mmHg ± 19.4 at the three examinations respectively, and HR was 77 beats per minute (BPM) ± 12, 71 BPM ± 8 and 74 BPM ± 9. PWV was 6.3 m/s ± 2.19, 5.7 m/s ± 0.6 and 5.9 m/s ± 1.4, respectively. There was no significant effect of examination day, MAP, or HR on PWV, evaluated by analysis of variance. Mean inter-examination coefficient of variation was 16%.

**Conclusion:** Assessment of PWV is feasible in anesthetized Göttingen minipigs, and therefore could have perspectives in a porcine model of atherosclerosis. Furthermore, reference values from this study corresponded to PWV values obtained from infants or young human individuals.

#### P2.17

##### EGENOGENICITY OF THE COMMON CAROTID ARTERY INTIMA-MEDIA COMPLEX IN STROKE

K. Aizawa<sup>1,2</sup>, S. Elyas<sup>1,2</sup>, D. D. Adingupu<sup>1,2</sup>, A. C. Shore<sup>1,2</sup>, W. D. Strain<sup>1,2</sup>, P. E. Gates<sup>1,2</sup>

<sup>1</sup>University of Exeter Medical School, Exeter, United Kingdom

<sup>2</sup>NHR Exeter Clinical Research Facility, Exeter, United Kingdom

**Introduction:** Grey scale median of the carotid artery intima-media complex (IM-GSM) is a recently introduced measurement thought to reflect the composition of the arterial wall. Carotid artery intima-media thickness (IMT) has been shown to be a predictor of a future stroke incidence, but the relationship between IM-GSM and stroke is unclear. This study therefore examined IM-GSM in individuals with stroke.

**Methods:** Fifty-seven healthy individuals (CONTROL: 64.1±7.8yrs, 26F) and 96 individuals with cerebrovascular disease (either stroke or transient ischemic attack) diagnosed within 3 months before the study visit (CRVD: 68.6±9.8yrs, 30F) were included in this study. Common carotid artery diameter and far-wall IMT images were obtained using a Doppler ultrasound machine. IMT and IM-GSM were analyzed using semi-automated edge-detection software.

**Results:** Carotid diameter and IMT were greater in CRVD than CONTROL (all  $p < 0.005$ ). IM-GSM was significantly higher in CONTROL than CRVD (119.5±27.3au vs 105.8±30.3au,  $p < 0.01$ ). IMT and IM-GSM were similar between the carotid arteries of the affected and unaffected sides in CRVD. In a pooled data set, there was a significant reduction in IMT ( $r = -0.53$ ) and wall-to-lumen ratio (WLR;  $r = -0.50$ ) with the increase in the quartiles of IM-GSM (both  $p < 0.001$ ).

**Conclusion:** These results demonstrate that IM-GSM was lower in CRVD than CONTROL, and the level of IM-GSM appeared to be systemic in CRVD. The inverse association observed between IMT, WLR and IM-GSM may suggest an alteration in carotid artery wall composition with the degree of arterial remodelling.

#### P2.18

##### TOWARDS COMPUTATIONAL DIAGNOSIS OF CORONARY ARTERY DISEASE

S. Shaw<sup>1</sup>, J. R. Whiteman<sup>1</sup>, S. E. Greenwald<sup>2</sup>, C. Kruse<sup>1</sup>, H. T. Banks<sup>5</sup>, M. J. Birch<sup>3</sup>, Z. R. Kenz<sup>5</sup>, J. Reeves<sup>3</sup>, S. Hu<sup>5</sup>, M. P. Brewin<sup>4</sup>

<sup>1</sup>Brunel University, Uxbridge, United Kingdom

<sup>2</sup>Queen Mary University, London, United Kingdom

<sup>3</sup>Barts Health National Health Service Trust, London, United Kingdom

<sup>4</sup>Salisbury District Hospital, Salisbury, United Kingdom

<sup>5</sup>North Carolina State University, Cary, United States of America

Flow in the wake of a coronary artery stenosis induces a bruit in the 300-1500 Hz range that can be heard at the chest wall. It has been hypothesised that this sound is caused by turbulence-induced shear waves which travel through the soft tissue of the thorax. This contribution describes a computational mathematical 'forward solve' method to simulate these shear waves in a virtual chest of tissue mimicking agarose gel. As the first stage in the development of a noninvasive diagnostic tool we also describe initial results towards the solution of the mathematical inverse problem. That is: to identify the source of the bruit given the surface measured signal.

**Objectives:** To demonstrate proof-of-concept of a novel biotechnology that will use mathematical simulations to provide a non-invasive screening tool for coronary artery disease.

**Methods:** Finite element based forward solvers for soft tissue response (given the source, generate the signal); optimisation-based inverse solver (given the signal, determine the source).

**Results:** For a simple, small scale, and axisymmetric cylindrical gel configuration, and for a source at 500 Hz, the forward solve generates signals that agree with experimental data (using Kelvin-Voigt viscoelasticity). Also, with surface signals generated by simulated sources in this virtual environment the inverse algorithm is able to identify this source given only chest surface measurements, and an adequate initial datum from which to start the computation.

**Conclusions:** While enormous challenges remain we have shown that this approach offers considerable promise in delivering a noninvasive diagnostic or screening tool.

#### P2.19

##### ASSESSMENT OF AORTIC PULSE WAVE VELOCITY BY ULTRASOUND: A FEASIBILITY STUDY IN MICE

N. Di Lascio <sup>1</sup>, F. Stea <sup>1,2</sup>, C. Kusmic <sup>1</sup>, S. Cintoli <sup>3</sup>, R. Sicari <sup>1</sup>, F. Faita <sup>1</sup>

<sup>1</sup>Institute of Clinical Physiology, National Council of Research, Pisa, Italy

<sup>2</sup>Department of Internal Medicine, University of Pisa, Pisa, Italy

<sup>3</sup>Istituto di Neuroscienze, Consiglio Nazionale delle Ricerche (CNR), Pisa, Italy

Pulse wave velocity (PWV) is considered a surrogate marker of arterial stiffness and could be useful for characterizing cardiovascular disease progression even in mouse models. Aim of this study was to develop an image process algorithm for assessing arterial PWV in mice using ultrasound (US) images only and test it on the evaluation of age-associated differences in abdominal aorta PWV (aaPWV). US scans were obtained from six adult (7 months) and six old (19 months) wild type male mice (strain C57BL6) under gaseous anaesthesia. For each mouse, diameter and flow velocity instantaneous values were achieved from abdominal aorta B-mode and PW-Doppler images; all measurements were obtained using edge detection and contour tracking techniques. Single-beat mean diameter and velocity were calculated and time-aligned, providing the lnD-V loop. aaPWV values were obtained from the slope of the linear part of the loop (the early systolic phase), while relative distension (relD) measurements were calculated from the mean diameter signal. aaPWV values for young mice ( $3.5 \pm 0.52$  m/s) were lower than those obtained for older ones ( $5.12 \pm 0.98$  m/s) while relD measurements were higher in young ( $25\% \pm 7\%$ ) compared with older animals evaluations ( $15\% \pm 3\%$ ). All measurements were significantly different between the two groups ( $P < 0.01$  both). In conclusion, the proposed image processing technique well discriminate between age groups. Since it provides PWV assessment just from US images, it could represent a simply and useful system for vascular stiffness evaluation at any arterial site in the mouse, even in preclinical small animal models.

#### P2.20

##### ACOUSTIC LOCALISATION OF CORONARY ARTERY STENOSIS: WAVE PROPAGATION IN SOFT TISSUE MIMICKING GELS

S. E. Greenwald <sup>1</sup>, H. T. Banks <sup>2</sup>, M. J. Birch <sup>3</sup>, M. P. Brewin <sup>3</sup>, S. Hu <sup>2</sup>, Z. R. Kenz <sup>2</sup>, C. Kruse <sup>4</sup>, D. Mehta <sup>1</sup>, J. Reeves <sup>3</sup>, S. Shaw <sup>4</sup>, J. R. Whiteman <sup>4</sup>

<sup>1</sup>Pathology Group, Blizzard Institute, Barts & The London School of Medicine & Dentistry, London, United Kingdom

<sup>2</sup>Center for Research in Scientific Computation, North Carolina State University, Raleigh, United States of America

<sup>3</sup>Clinical Physics, Barts Health National Health Service Trust, London,

United Kingdom

<sup>4</sup>BICOM, Brunel, University, Uxbridge, United Kingdom

**Background:** Turbulent flow downstream of atherosclerotic plaques produces low amplitude shear waves which travel through the chest and can be measured by skin sensors. This acoustic signature may provide a cheap non-invasive way to diagnose arterial disease. We report measurements of shearing oscillations and flow-induced turbulence in soft tissue-mimicking gels which provide input to a numerical model of soft tissue behaviour described in a companion presentation.

**Methods:** Cylindrical specimens of 3% agarose gel were cast around an axial rod and bead connected to an electromechanical vibrator (figure 1), to generate shear-waves of known characteristics and location (frequency 250-750 Hz, amplitude 10-50  $\mu$ m). Displacement was mapped optically by tracking the movement of carborundum particles on the surface. In the flow study (figure 2) a silicone rubber tube (i.d. 4.5mm) containing a stenosis was embedded in a cuboidal gel phantom and lateral displacement of the gel surface was mapped by a piezo-electric accelerometer.

**Results:** Forced oscillations produced movement in the same direction at the gel surface, amplitude 10-50% of the bead's movement. Amplitude modulation ( $\approx 5\%$ ) at around 40Hz, probably due to resonance in the gel, was also seen. Lateral movement (200-800Hz) of the gel surface caused by flow-induced turbulence increased monotonically with turbulence magnitude.

**Conclusions:** The methods described above provide internally consistent and repeatable data, validating the numerical models. The next steps will compare computational results with measurements in progressively more realistic representations of the chest aiming ultimately to produce a device suitable for screening/diagnosis of coronary artery disease.

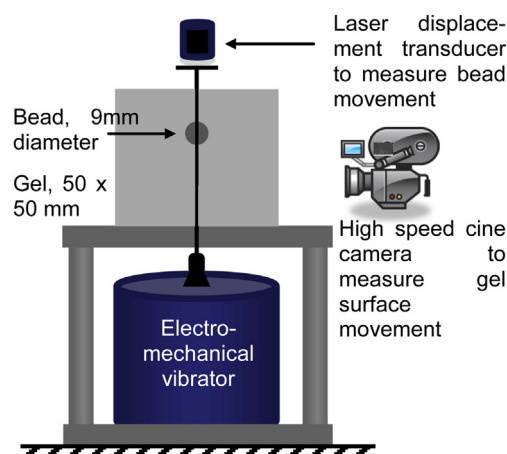


Figure 1. Forced vibration rig. Gels cast with bead in various positions. Laser measures bead movement; camera measures surface movement

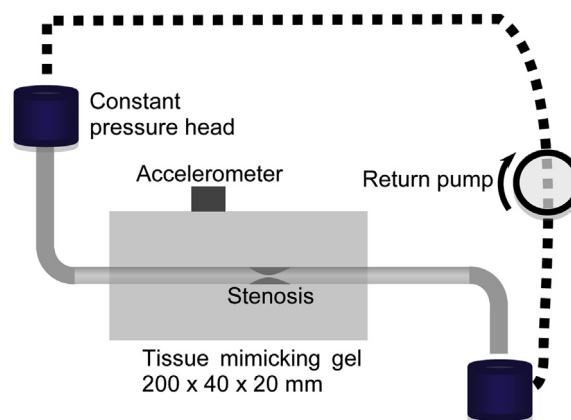


Figure 2. Steady flow rig. Measurements made at various flow rates, tube depths and stenosis severity. Accelerometer position varied.